Fast MRI evaluation of pulmonary progressive massive fibrosis with VIBE and HASTE sequences: comparison with CT

Koray Hekimoğlu, Tanzer Sancak, Meltem Tor, Halit Beşir, Bora Kalaycıoğlu, Sadi Gündoğdu

PURPOSE
The aim of this prospective study was to evaluate the diagnostic utility of volumetric interpolated breath-hold examination (VIBE) and half-Fourier-acquisition single-shot turbo spin-echo (HASTE) fast magnetic resonance imaging (MRI) sequences in the evaluation of pulmonary progressive massive fibrosis (PMF) in comparison with computed tomography (CT) imaging. If fast MRI is proven to be diagnostically significant, this modality can be used for diagnosis and follow-up studies of PMF patients.

MATERIALS AND METHODS
Twenty-two PMF lesions from 20 coal workers were evaluated. After CT imaging, patients underwent pre-contrast VIBE, contrast-enhanced VIBE, and HASTE MRI studies for detection and evaluation of the PMF lesions. Measurements of the three groups were evaluated with intra-class coefficients. Correlation levels between sizes, image quality, and artifact were evaluated with linear Pearson correlation analysis.

RESULTS
There was almost perfect agreement among radiologists for lesion detection with kappa analysis. There was significant agreement between three MRI study groups and gold standard CT images. We found the best agreement values with contrast-enhanced VIBE images for lesion detection and image quality in comparison with CT imaging. Presence of artifact was also lowest with this protocol.

CONCLUSION
With fast MRI sequences in pulmonary imaging, image quality has significantly improved being very close to that of CT studies. In this study, contrast-enhanced VIBE protocol provided the best depiction of PMF lesions. This protocol may be an alternative choice for CT, avoiding the use of iodinated contrast material and minimizing exposure to ionizing radiation for follow-up studies.

Key words: • pulmonary fibrosis • magnetic resonance imaging • computed tomography • comparative study

Progressive massive fibrosis (PMF) of the lung is a type of late stage pneumoconiosis and pathologically consists of fibrotic lesions more than 1 cm in greatest diameter (1). The chest radiographic and computed tomography (CT) findings of PMF have been reported (2, 3). In our geographic region, PMF is mostly seen as a complication of coal workers' pneumoconiosis (CWP). Evaluation and follow-up of PMF lesions are generally performed by using CT scans in CWP patients. However, imaging has to provide detailed information about the anatomical extension of the PMF. Since CT imaging requires ionizing radiation and application of CT contrast agents is limited in patients with allergies to ionized contrast media or in patients with renal insufficiency, alternative imaging methods for diagnosis and follow-up are always of interest. If the fast magnetic resonance imaging (MRI) of PMF lesions of the lungs is proven to be diagnostically significant, this modality can be used instead of CT imaging. The rapid development of MRI techniques during the last years has resulted in excellent soft tissue imaging capabilities. MRI of the lung is difficult and hampered by three factors: first (and very important) is signal loss due to physiological motion (respiration and cardiac pulsation); second is low proton density in lung results in a low signal-to-noise-ratio (SNR); and third is the unique combination of air and soft tissue resulting in significant susceptibility to artifact. Despite these difficulties, fast MRI techniques for evaluating lung pathology have been developed and addressed in a number of articles describing preliminary results (4–6). However, correct evaluation of PMF lesions by fast MRI techniques has not yet been well described. Volumetric interpolated breath-hold examination (VIBE) and half-Fourier single-shot turbo spin echo (HASTE) MR sequences are very fast imaging techniques, and these techniques can also be used for fast pulmonary imaging.

In the present study, we hypothesized that fast pulmonary MRI of the PMF lesions by using VIBE and HASTE fast MRI protocols would enable detection of lesions and might have a role in the management of PMF, especially in long-term follow-up. Thus, the purpose of our study was to determine the feasibility of fast MRI in the management of PMF in comparison with CT imaging.

Materials and methods

Study design

Twenty-three patients were enrolled in this prospective study between January 2007 and July 2008. Three patients were unable to undergo MRI because of claustrophobia and had to be excluded from the study. Thus, data sets of 20 patients were analyzed for this study. All patients were male, with an age range of 52–82 years (mean, 72 years). The patients had worked as coal miners for 15–25 years (mean, 15 years) working underground. They had pulmonary mass lesions rang-

From the Department of Radiology (K.H. ✉ korayhekim@yahoo.com.tr), Başkent University School of Medicine, Ankara, Turkey; the Department of Radiology (T.S., S.G.), Ufuk University School of Medicine, Ankara, Turkey; the Departments of Pulmonary Diseases (M.M.) and Radiology (H.B., B.K.), Karaelmas University School of Medicine, Zonguldak, Turkey.

ing from 25 mm to 50 mm in diameter (mean, 35 ± 3 mm) on CT images. Transthoracic biopsy was applied to all lesions by interventional radiology department, and PMF diagnosis was histopathologically confirmed. Follow-up of the PMF lesions in these patients were performed with CT. We selected lesions that showed no significant change on CT for at least 2 years in order to exclude the possibility of a coexistent lung cancer.

One week after CT study, all patients underwent a pre-contrast VIBE, HASTE, and contrast-enhanced VIBE MRI for the evaluation of the PMF lesions. Both MRI and CT examinations were well tolerated with no adverse reactions. None of the data sets were excluded for serious respiratory or motion artifact, and no examination had to be repeated because of poor image quality. The mean in-room time was 10 ± 5 min for MRI examination and 8 ± 2 min for CT examination.

Images were divided into four groups for each patient (Group I, CT images; Group II, pre-contrast VIBE images; Group III, contrast-enhanced VIBE images; and Group IV, HASTE images). Upon completion of imaging in every patient, all imaging groups were interpreted by five experienced radiologists. Measurement of lesions on each imaging sequence was performed for further statistical analysis.

This study was approved by the institutional ethics committee of Karaelmas University School of Medicine. Informed consent was obtained from all patients.

Imaging techniques

CT scans were performed on spiral CT (Philips Secura 2000, Philips Medical Systems, Best, The Netherlands) using the following parameters: 120 kV; 150 mA; pitch factor, 1,5; slice width, 7 mm; effective slice thickness and reconstruction, 5 mm; in-plane matrix size, 512 × 512. A contrast agent (100 mL iopromide [300 mgI/mL, Ultravist, Schering AG, Berlin, Germany]) was used with CT injector system (Medrad Vistron CT injection system, Medrad Inc., Warrendale, Pennsylvania, USA) via vena brachialis with 3 mL/s flow rate. After a delay of 30 s, the image set covering the entire lung was collected over 12–15 s. This protocol is our standard for routinely performed thoracic CT.

MRI was performed with two 1.5 T MRI scanners (Intera Master Gyroscan, Philips Medical Systems, Best, The Netherlands; and Magnetom Symphony, Siemens Medical Solutions, Erlangen, Germany) with a maximum gradient strength of 30 mT/m and a slew rate of 150 mT/m per ms. A standard phased-array body coil was used for signal reception. ECG triggering with an active fiberoptic ECG system was used for reduction of cardiac motion artifact in HASTE sequence imaging. Seventeen patients were scanned with the Philips scanner, and the remaining three with the Siemens scanner.

Fast T1-weighted MRI sequences

T1-weighted VIBE sequence was chosen for fast T1-weighted MRI. VIBE sequence parameters were adapted to Philips scanner for the ultrafast 3D gradient echo (T1-TFE) sequence. Imaging parameters for VIBE sequence were as follows: TR/TE, 5.12/2.51 ms; flip angle, 10°; partition thickness, 5 mm without interslice gaps; matrix size, 256 × 116 with three-dimesional (3D) breath-hold imaging technique. The 3D VIBE sequence is a 3D-gradient echo (GRE) sequence (volumetric interpolated breath-hold examinations) and has been presented as a fast MR sequence for liver and pulmonary imaging. It is similar to the 3D radiofrequency-spoiled GRE sequence used to perform 3D MR angiography. However, this sequence differs from MR angiography sequences by symmetrical k-space acquisition in the phase encoding and the partition encoding directions (k_y and k_z, respectively), which decreases truncation artifact and improves image quality. On the other side, ultrafast spoiled gradient echo (T1-TFE) sequence was used on Intera-Philips scanner for fast T1-weighted MRI with these parameters: TR/TE, 4.67/1.67 ms; flip angle, 20°; matrix size, 256 × 192. Fat saturation techniques were not employed. The field of view (FOV) ranged from 375 mm to 450 mm for the acquisition of coronal and axial MRI images for the two MRI scanners. Breath-hold protocol was applied for better image contrast. Acquisition time was 20 s. Pre- and post-contrast images were obtained in all patients. We used a power injector (Medrad Vistron MR injection system, Medrad Inc.) to inject 0.1 mmol/kg of gadopentate dimeglubine (Magnevist,

Schering AG) at a rate of 2 mL/s in all patients. Contrast-enhanced MR images were obtained 60–70 s after completion of the intravenous injection.

Fast T2-weighted MRI sequences

T2-weighted HASTE was used for fast T2-weighted MRI. The HASTE sequence is described as a useful breath-hold fast T2 imaging process in lung parenchyma. In HASTE sequence, the data were acquired during a train of 180° refocusing pulses. The central portion of k-space was acquired immediately after the radiofrequency (RF) pulse, and image reconstruction was performed with a half-Fourier method by using k-space symmetry. ECG triggered, breath-hold, black blood (SPIR) prepared HASTE images were obtained in the axial and coronal orientation with the following parameters: TR/TE, 2000 (2 R-R intervals)/53 ms; flip angle, 160°; effective slice thickness, 5 mm without interslice gaps; matrix size, 256 × 256; NSA, 3; phase-encoding direction, anteroposterior. In HASTE scanning, 35 slices covering the entire lung area were collected in two interleaved concatenations of 20 s for each set. No contrast agent was given. For patients evaluated with the Philips Intera scanner, this sequence was adapted as being single-shot turbo spin echo (TSE) sequence with the following parameters: TR/TE, 2000/80 ms; effective slice thickness, 5 mm without interslice gaps; matrix size, 256 × 192; turbo factor, 17 selected. FOV range was 375–400 mm for these sequences. The T2 TSE sequence was combined with spectrally selective attenuated inversion recovery (SPAIR) for fat saturation.

Image analysis

The analysis of the imaging data was performed in a four-step manner after completion of data acquisition for all patients. It was based on reviewing hard and soft copies, which were available on workstations for the two MRIs.

In step 1 of the analysis, the gold standard reference images were defined by two experienced radiologists in consensus by reviewing and interpreting the CT scans. They remained blinded to the MRI findings of these patients. All PMF lesions previously confirmed by biopsy were counted for the study. The number, location, and three dimensional sizes of the detected lesions (transverse, sagittal, and craniocaudal

diameters) were recorded (Group I). To avoid miscounting, the observers marked each detected lesion on hard-copy film.

In step 2 of the analysis, each MRI group was analyzed independently by two experienced radiologists who were unaware of the results of the CT examinations. Each radiologist recorded the sizes, number, and location of PMF lesions on each MR image.

In step 3, the corresponding CT and MRI data sets were reviewed again simultaneously for one-to-one comparison of the size and location of the detected lesions in all groups of images for each patient. Three radiologists independently evaluated the general image quality (A) and presence of artifact (B) of detected pulmonary lesions. In the grading of image quality (A), radiologists used a semiquantitative grading system as follows: 1 = poor (images which are non-diagnostic), 2 = fair (not optimal quality but sufficient to permit a diagnosis to be established), 3 = good (optimal image quality in resolution, sharpness, and clarity), and 4 = excellent (best image quality). All MRI images (Groups II–IV) were evaluated with regard to artifact (B) caused by breathing or cardiac pulsation separately. Total artifact scores were also calculated. In all patients, each lobe of the lung and PMF lesions were scored for the presence of artifact (score 0, no artifact; score 1, minor artifact; score 2, moderate artifact; score 3, severe artifact with insufficient imaging quality for diagnosis).

In step 4 of the image analysis, PMF lesions were evaluated for signal and post-contrast enhancement patterns of the lesions by two radiologists in consensus by reviewing the MRI images. The pre-contrast signal intensity (SI) was supposed to reflect the status of massive fibrosis, and the signal pattern including post-contrast enhancement was supposed to reflect the secondary change or vascular nature of PMF. Quantitative analysis was not performed in this study because the region of interest (ROI) measurements showed considerable variability of SI within the same lesion in the pilot study. In this analysis, the relative intensities of PMF lesions were compared with skeletal muscle on the same MRI images and categorized as hypointense, isointense, or hyperintense.

Contrast-enhanced VIBE images (Group III) were classified into three patterns: (a) no enhancement, (b) rim enhancement, and (c) diffuse enhancement. Contrast enhancement of the PMF lesions was defined visually as increase of SI after intravenous administration of contrast media at the same contrast window and level setting. On the other side; the signal pattern of lesions on pre-contrast VIBE and HASTE images (Groups II, IV) were classified into four types: (a) homogenous isointense SI, (b) homogenously low SI, (c) high SI only at the rim, and (d) high SI areas and high SI rim.

Statistical analysis

All results were statistically described using commercial software (SPSS 11, SPSS Inc., Chicago, lllinois, USA; Excel 2003, Microsoft, Redmond, Washington, USA). Type I error was accepted as 0.05, All reported *P* values were type-3 Wald significance levels and were declared to indicate a statistical significance if <0.05. Measurement of the results in three groups (II, III, IV) on three sizes were evaluated with intra-class coefficient (ICC). Correlation levels between these results and gold standard CT results (Group I) were evaluated with linear Pearson correlation analysis. The significance of differences between groups were determined with randomized block design for artifacts. In addition, group differences in image quality and spatial resolution were calculated using Friedman test. Simple kappa coefficients were used to assess interobserver agreement for lesion detection (0.00–0.20 indicated slight agreement; 0.21–0.40 fair agreement; 0.41–0.60 moderate agreement; 0.61–0.80 substantial agreement; and 0.81–1.00 almost perfect agreement).

Results

Diagnoses based on imaging findings

Twenty-two PMF lesions were identified and evaluated in 20 patients with CT and MRI. Based on the one-to-one correlation between CT and MR images, the findings in all imaging techniques correlated well. All MRI images were of acceptable diagnostic quality. However, the image quality of lung parenchyma and PMF lesions was better detected with contrast-enhanced VIBE images than pre-contrast VIBE and HASTE images (Figs. 1–3). MRI interpretations did not show false-negative

or false-positive findings. None of the lesions detected on CT were missed on MRI images.

*Evaluation of measurements on imaging findings*

Linear correlation of the results between Group I (gold standard CT images) and the other groups (II-IV) which were pre-contrast VIBE, post-contrast VIBE, and HASTE sequence images respectively, were evaluated for three dimensions of the lesions. Correlation (r) values for x dimension between Group I and the other groups (II–IV) were 0.972, 0.989, and 0.829, respectively. With respect to y dimension, r values were 0.987, 0.996, and 0.862, respectively. Finally, r values for z dimension between Group I and the other groups were calculated as 0.997, 0.999, and 0.959, respectively. For all correlations *P* values were <0.01. Agreement values (ICC) for each dimension between three study groups and gold standard Group I are shown in Table 1. We found significant agreement between three study groups (II–IV) and gold standard Group I. Best agreement with gold standard CT imaging values for r and ICC were obtained with Group III (post-contrast VIBE sequence studies).

Interobserver agreement

There was almost perfect agreement among radiologists regarding report quality for both the CT lesion detection group (kappa score, 0.85) and for the MRI lesion detection group (kappa score, 0.83).

Image quality

In all study groups, post-contrast VIBE (Group III) images had the best diagnostic quality. For Group III, average quality score (± standard deviation, SD) was 3.65 ± 0.49 with a median value of 4 (excellent). Pre-contrast VIBE (Group II) images had the second best diagnostic quality; statistical values for this group were 3.2 ± 0.41 with a median value of 3 (good). HASTE (Group IV) images did not have a high diagnostic quality. Degradation was observed on these images because of respiratory or cardiac motion artifact and short scan times. The average quality score for Group IV was 2.25 ± 0.44, with a median value of 2 (poor). All groups had statistically significant differences with each other (*P* < 0.01).
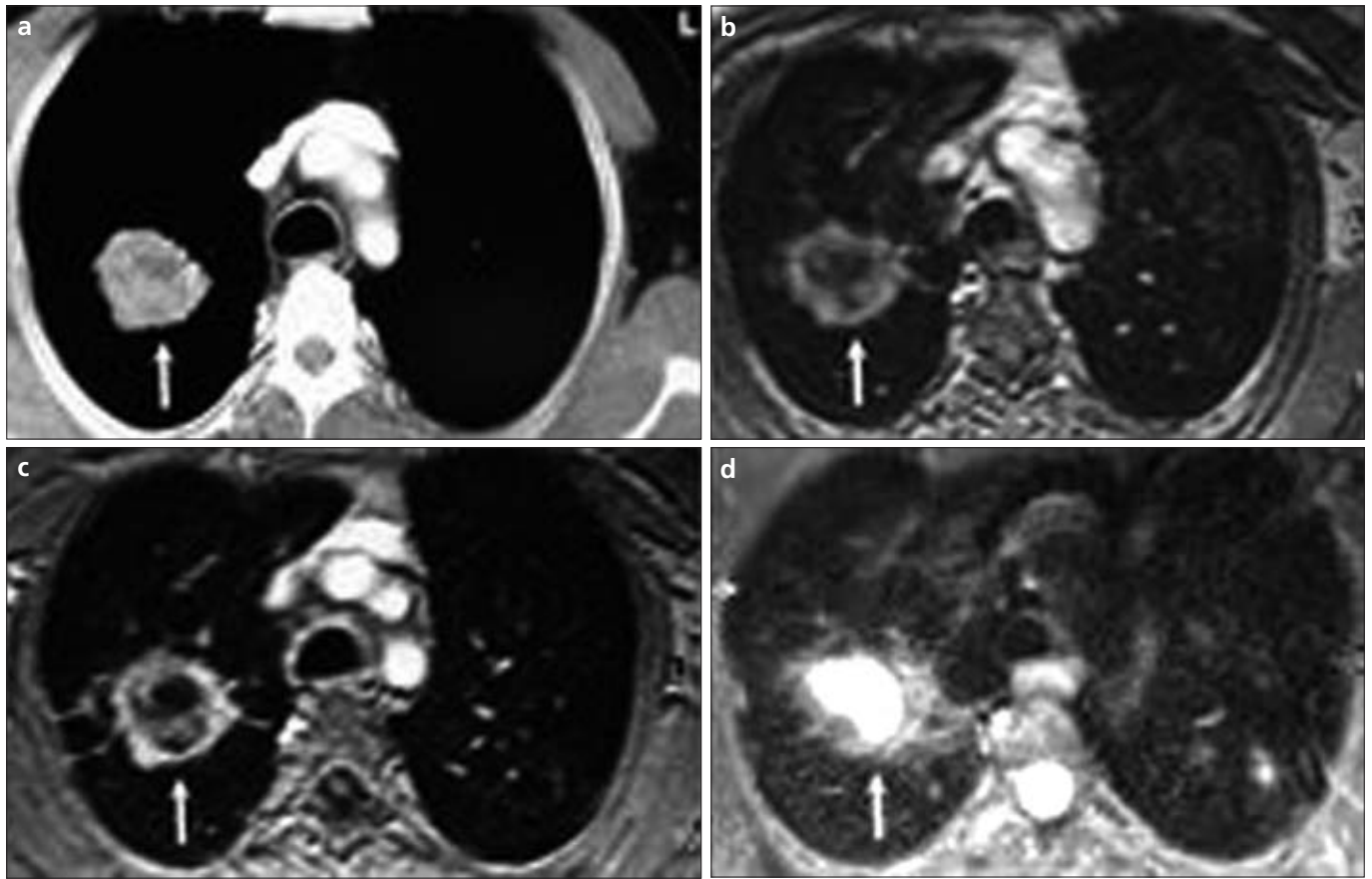
Figure 1. a–d. Axial plane CT **(a)**, pre-contrast VIBE **(b)**, contrast-enhanced VIBE **(c)**, and HASTE MR **(d)** images of a 47-year-old coal worker who presented with huge progressive massive fibrosis lesion on the right side *(white arrows)*.

Artifacts

With regard to comprehensive scoring of breathing and cardiac pulsation artifacts, post-contrast VIBE scans provided the lowest artifact scores compared with the pre-contrast VIBE and HASTE sequences in all parts of the lung. The average total artifact score ranged from 0.1 to 1 for pre-contrast VIBE (Group II) images, from 0.1 to 1 for post-contrast VIBE (Group III) images, and from 0.8 to 1.8 for HASTE (Group IV) images.

In all MRI sequences, respiratory artifact was more prominent than cardiac or vessel pulsation artifact. This may be related to our breath-hold choice while determining MRI sequences. Pulsation and cardiac artifact ranged from 0 to 0.8 for pre-contrast VIBE (Group II), from 0 to 0.8 for post-contrast VIBE (Group III) images, and from 0.8 to 1.8 for HASTE (Group IV) images. Respiratory artifact ranged from 0.1 to 1.2 in Group II for pre-contrast VIBE images from 0.1 to 0.8 in Group III for post-contrast VIBE sequence, and from 0.8 to

Table 1. Intra-class coefficients (ICC) between gold standard (Group I) and the other groups for "x", "y", and "z" dimensions (single measures ICC)

	Group II	Group III	Group IV
"x" dimension			
Group I	0.967	0.989	0.774
P values	<0.0001	<0.0001	<0.0001
"y" dimension			
Group I	0.982	0.996	0.784
P values	<0.0001	<0.0001	<0.0001
"z" dimension			
Group I	0.990	0.999	0.873
P values	<0.0001	<0.0001	<0.0001

Group I, CT images; Group II, pre-contrast VIBE images; Group III, contrast-enhanced VIBE images; Group IV, HASTE images.

1.8 for Group IV (HASTE) images. We did not find significant differences in artifact between Group II and III images. However, we found a significant difference between group IV and other groups (II–III) (*P* < 0.05). Average artifact scores in different pulmonary locations are shown in Table 2.

Signal intensity

On pre-contrast VIBE images (Group II), homogenous isointense SI compared with skeletal muscle (n = 16, 72%) was the most frequent SI, followed by homogenous low SI (n = 2, 9%), and high SI rim only (n = 2, 9%). The PMF lesions did not show
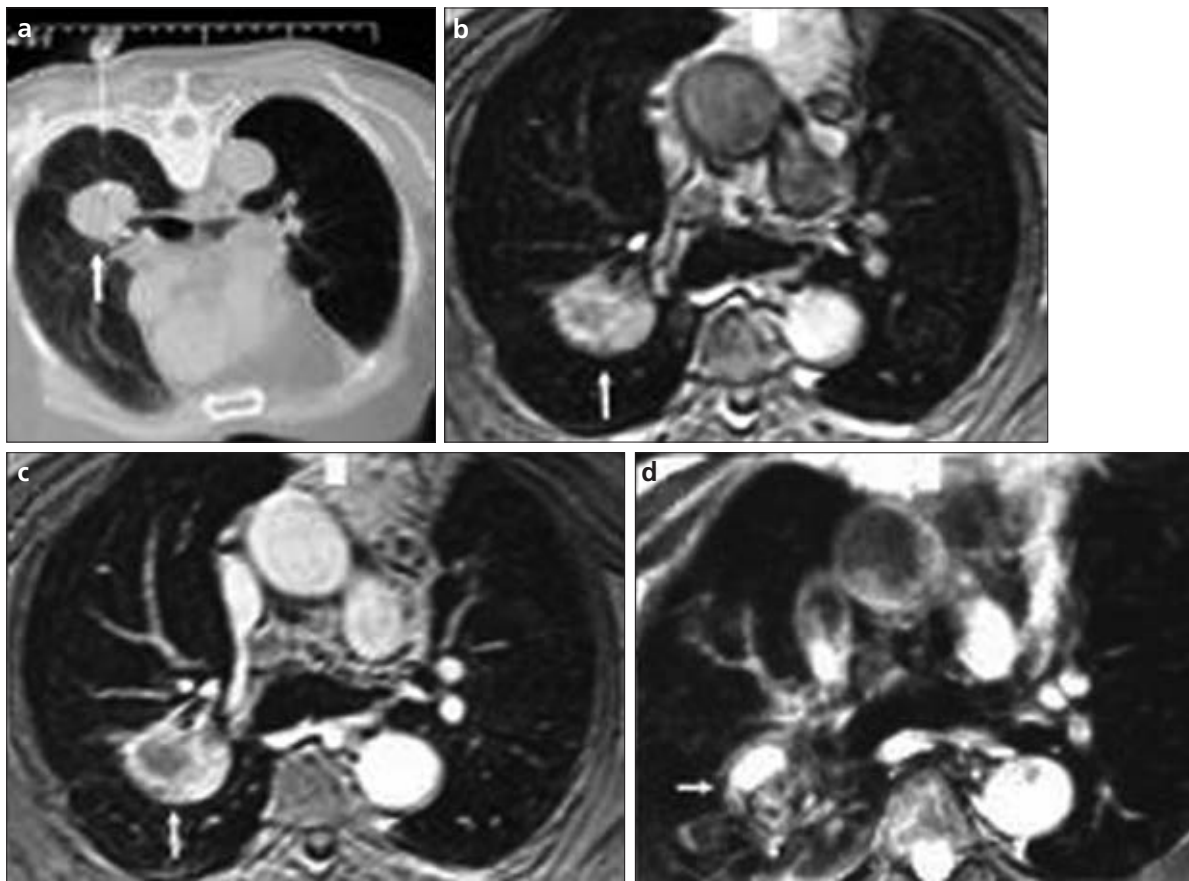
Figure 2. a–d. CT-guided biopsy **(a)**, pre-contrast VIBE **(b)**, contrast-enhanced VIBE **(c)**, and HASTE MR **(d)** images of a 55-year-old coal worker who had large progressive massive fibrosis lesion on the right lower lobe *(white arrows)*. The lesion showed diffuse enhancement pattern on contrast-enhanced image **(c)** with excellent image quality and minor artifact scores.

Table 2. Average artifact score as found in the study groups in different pulmonary localizations

	Pulsation-cardiac artifacts			Breathing artifacts			Total artifacts		
	Group II	Group III	Group IV	Group II	Group III	Group IV	Group II	Group III	Group IV
Right upper lobe	0	0	1	0.1	0.1	1	0.1	0.1	1
Right middle lobe	0	0	1.4	0.2	0.2	1.6	0.2	0.2	1.5
Right lower lobe	0.2	0.2	1.8	0.5	0.4	1.8	0.4	0.3	1.8
Left upper lobe	0	0	1.5	0.1	0.1	1.5	0.1	0.1	1.5
Left lower lobe	0.2	0.2	1.8	0.5	0.4	1.8	0.4	0.3	1.8
Hilar zone	0.6	0.6	1.4	0.3	0.2	1.5	0.5	0.4	1.5
Mediastinum	0.8	0.8	0.8	1.2	0.8	0.8	1	1	0.8
PMF lesions	0	0	1	0.1	0.1	1	0.1	0.1	1

Group II, pre-contrast VIBE images; Group III, contrast-enhanced VIBE images; Group IV, HASTE images.
Artifact scoring: Score 0, no artifacts; score 1, minor artifacts; score 2, mild artifacts; score 3, severe artifacts. PMF, progressive massive fibrosis.

both high SI areas and high SI rim in this group. On HASTE images (Group IV), the PMF lesions showed mostly homogenous low SI (n = 20, 91%), and the other lesions showed iso-intense SI (n = 2, 9%). PMF lesions did not show high SI rim at the rim only or in the lesion and at the rim in Group IV. In evaluation enhancement patterns, Group III showed rim enhancement in 10 PMF lesions (45%) and diffuse enhancement in the other 12 lesions (55%). There were no non-enhancing PMF lesions in this group (Table 3).

Discussion

In this study, we combined two fast MRI sequences for evaluating PMF lesions. T1-weighted VIBE sequence was performed pre- and post-contrast enhancement. The gold standard modality for evaluating pulmonary lesions is spiral or multidetector CT,
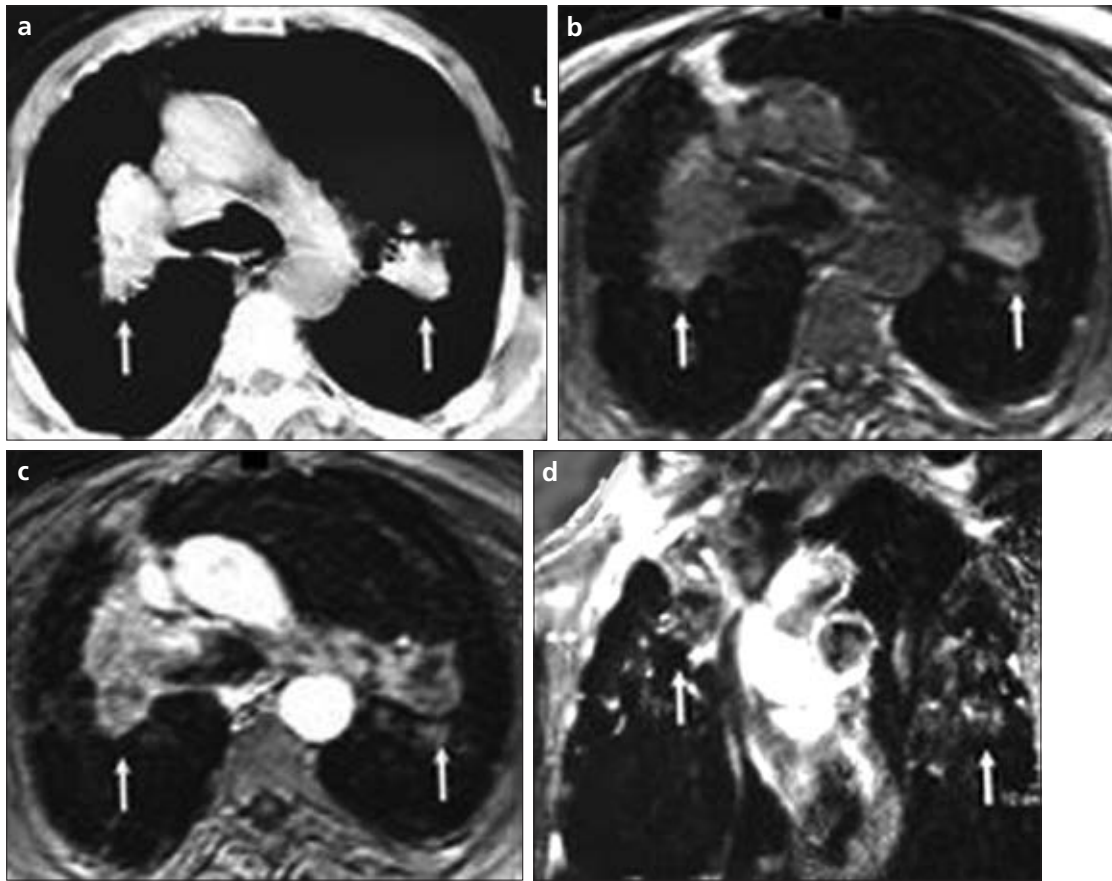
Figure 3. a–d. Axial plane CT (**a**), pre-contrast VIBE (**b**), and contrast-enhanced VIBE MR (**c**) images of a 52-year-old coal worker with a 20-year underground working history who had progressive massive fibrosis lesions on each lung *(white arrows)*. The lesion revealed rim enhancement pattern on coronal post-contrast MR image (**d**, *white arrows*).

Table 3. Qualitative analysis of images for signal and enhancement patterns (number/total number of lesions and percentage)

	Group II		Group III		Group IV	
Signal pattern						
Homogenous iso SI	16/22	72%			2/22	9%
Homogenous low SI	2/22	9%			20/22	9%
High SI rim	2/22	9%			-	-
High SI rim and high SI areas	-	-			-	-
Enhancement pattern						
No enhancement			-	-		
Rim enhancement			10/22	45%		
Diffuse enhancement			12/22	55%		

Group II, pre-contrast VIBE images; Group III, contrast-enhanced VIBE images; Group IV, HASTE images. SI, signal intensity.

although several studies have presented MRI assessment of pulmonary lesions as a similarly efficient modality (5–9).

PMF is defined as a lesion of fibrosis and pigment deposition larger than 1 cm in diameter and is sometimes designated as "complicated" pneumoconiosis. These lesions commonly occur in coal workers who have had exposure to large amounts of heavy dust. Radiologically, PMF starts near the periphery of the lung and may closely resemble pulmonary carcinoma (2, 6, 10).

According to the results of this study, results of fast MRI in PMF patients may be identical to results of CT, which is accepted as gold standard in pulmonary pathologies. Compared with the pre-contrast VIBE and HASTE images, the contrast-enhanced VIBE images provided superior visualization of PMF lesions in pulmonary parenchyma. These results show that post-contrast VIBE sequence imaging has the best agreement with gold standard CT imaging.

VIBE sequence is a 3D gradient-echo MRI technique tailored toward minimizing acquisition time and partial volume effects and maximizing image contrast, permitting imaging of tissue, with the first studies focusing on the liver (11). VIBE sequence has been proven to provide high spatial resolution, good visualization of lung anatomy, and low rates of artifact in healthy volunteers. These image qualities have been confirmed in recent studies using 3D-GRE sequences in a wide spectrum

of malignant and benign pulmonary diseases (4, 12). This technique involves two independent directions—perpendicular (phase-encoding) and parallel (partition-encoding) to the plane of excitation. Asymmetric sampling performed in each of the phase-encoding directions improves spatial resolution. The main advantages of the VIBE sequence are its ability to rapidly acquire a volumetric data set during a single breath-hold, which enables acquisition of contiguous thin-slice images with no interslice gap. Another important point of this sequence is the relative lack of phase artifact secondary to cardiac motion. This is achieved by the very short acquisition time for the central 10% of k-space, because this area of k-space contributes the most to image contrast but is most susceptible to phase artifact. The very short TR of VIBE sequence (4.67 ms) allows rapid imaging of lungs during one breath hold time. However, a short TE of only 1.67 ms minimizes susceptibility effects due to short $T2^*$ relaxation time of pulmonary parenchyma and increases the SNR, resulting in successful visualization of pulmonary parenchyma (13). The reduction in image artifact is another factor that improves image quality in this technique.

In this sequence, fat saturation techniques were not employed; it could have increased TR, which would have increased acquisition time and imaging artifact. Fat suppression was thought to improve visualization of the mediastinum, chest wall, and axilla for this sequence and was critical for the detection of the PMF lesions, which were seen as a focus of high signal intensity on the darkened background of suppressed fat.

HASTE sequence is a half-Fourier single-shot of TSE fast imaging MRI technique. This sequence has been reported to be a useful breath-hold T2-weighted sequence for imaging of the lung parenchyma (14). Because of its rapid data acquisition, HASTE imaging is relatively insensitive to motion artifact and may be particularly valuable in patients who are unable to hold their breath for a long acquisition period. HASTE images are characterized by high signal intensity in water-rich tissues. Thus, pulmonary lesions and vessels appear bright, whereas surrounding air-filled parenchyma display low signal intensity (15, 16). Distinct blur-ring artifact was seen on virtually all HASTE images, and the VIBE sequence had scores indicating a "minor" level, but the differences in artifact level were not significant. However, this limitation of image quality of HASTE images entailed lower sensitivities in lesion detection compared to VIBE sequence. Small PMF lesions could hardly be differentiated from vessels because of blurring (16).

Similar to CT, VIBE and HASTE techniques allow continuous data acquisition during a single breath-hold. In this study, the smallest lesion was 25 mm in diameter. No lesions in the three study groups were missed; thus, sensitivity for lesion detection was 100% in all groups. VIBE sequence, especially post-contrast studies, revealed values close to those of CT images (17). Evaluation of lesion size with HASTE sequence, however, did not show high accuracy compared to gold standard CT images. Although CT has been regarded as a standard reference technique for detection of pulmonary nodules, it is associated with a relatively high level of ionizing radiation—from 10 to 100 times as much as chest radiography (18). Fast MRI techniques may be particularly useful in patients who would otherwise be exposed to a substantial cumulative dose of radiation from undergoing repeated chest CT, such as our study patients in whom periodic chest CT follow-ups for PMF lesions had been requested for the purposes of ruling out lung cancer and/or of occupational compensation.

There were several limitations in this study. First, our study population was small. However, our intent was to show the feasibility of using the VIBE and HASTE sequences for fast pulmonary MRI. So the results were statistically significant for our hypothesis. Second, in post-contrast imaging we used single delay time and we did not choose dynamic MRI study because quantitative analysis of ROI measurements showed considerable variability within the same lesion. Thus, we did not use prolonged dynamic study of PMF lesions for SI evaluation.

In conclusion, using fast MRI sequences such as VIBE and HASTE have potential clinical utility for the MRI evaluation of PMF lesions in pneumoconiosis. Of these techniques, post-contrast VIBE modality significantly reduces artifact and better depicts the PMF lesions than pre-contrast VIBE and HASTE modalities. Although CT is a much more widely available modality, fast pulmonary MRI could be an alternative modality, particularly if minimizing exposure to ionizing radiation or avoiding the use of iodinated contrast material is of concern. Additional studies are warranted to establish the clinical value of fast pulmonary MRI in patients with various pulmonary diseases.

References

1. Gibbs AR. Occupational lung disease. In: Halsleton PS, ed. Spencer's pathology of the lung. 5th ed. New York: McGraw Hill, 1996; 461–504.
2. Williams JL, Moller GA. Solitary mass in the lungs of coal miners. Am J Roentgenol Radium Ther Nucl Med 1973; 117:765–770.
3. Soutar CA, Collins HP. Classification of progressive massive fibrosis of coalminers by type of radiographic appearance. Br J Indust Med 1984; 41:334–339.
4. Biederer J, Both M, Graessner J, et al. Lung morphology: fast MR imaging assessment with a volumetric interpolated breath-hold technique: initial experience with patients. Radiology 2003; 226:242–249.
5. Both M, Schultze J, Reuter M, et al. Fast T1- and T2-weighted pulmonary MR-imaging in patients with bronchial carcinoma. Eur J Radiol 2005; 53:478–488.
6. Jung JI, Park SH, Lee JM, Hahn ST, Kim KA. MR characteristics of progressive massive fibrosis. J Thorac Imaging 2000; 15:144–150.
7. Matsumoto S, Mori H, Miyake H, et al. MRI signal characteristics of progressive massive fibrosis in slicosis. Clin Radiol 1998; 53:510–514.
8. Kauczor HU, Kreitner KF. MRI of the pulmonary parenchyma. Eur Radiol 1999; 9:1755–1764.
9. Bruegel M, Gaa J, Woertler K, Waldt S, Hillerer C, Rummeny EJ. MRI of the lung: value of different turbo spin-echo, single-shot turbo spin-echo, and 3D gradient-echo pulse sequences for the detection of pulmonary metastases. J Magn Reson Imaging 2007; 25:73–81.
10. Matsumoto S, Miyake H, Oga M, Takaki H, Mori H. Diagnosis of lung cancer in a patient with pneumoconiosis and progressive massive fibrosis using MRI. Eur Radiol 1998; 8:615–617.
11. Rofsky NM, Lee VS, Laub G, et al. Abdominal MR imaging with a volumetric interpolated breath-hold examination. Radiology 1999; 212:876–884.
12. Bader TR, Semelka RC, Pedro MS, Armao DM, Brown MA, Molina PL. Magnetic resonance imaging of pulmonary parenchymal disease using a modified breath-hold 3D gradient-echo technique: initial observations. J Magn Reson Imaging 2002; 15:31–38.

13. Biederer J, Reuter M, Both M, et al. Analysis of artifacts and detail resolution of lung MRI with breath-hold T1 weighted gradient-echo and T2 weighted fast spin-echo sequences with respiratory triggering. Eur Radiol 2002; 12:378–384.

14. Hatabu H, Gaa J, Tadamura E, et al. MR imaging of pulmonary parenchyma with a half-Fourier single-shot turbo spin-echo (HASTE) sequence. Eur J Radiol 1999; 29:152–159.

15. Vogt FM, Herborn CU, Hunold P, et al. HASTE MRI versus chest radiography in the detection of pulmonary nodules: comparison with MDCT. AJR Am J Roentgenol 2004; 183:71–78.

16. Schroeder T, Ruehm SG, Debatin JF, Ladd ME, Barkhausen J, Goehde SC. Detection of pulmonary nodules using a 2D HASTE MR sequence: comparison with MDCT. AJR Am J Roentgenol 2005; 185:979–984.

17. Karabulut N, Martin DR, Yang M, Tallaksen RJ. MR Imaging of the chest using a contrast-enhanced breath-hold modified three-dimensional gradient-echo technique: comparison with two-dimensional gradient-echo technique and multidetector CT. AJR Am J Roentgenol 2002; 179:1225–1233.

18. Diederich S, Wormanns D, Lenzen H, Semik M, Thomas M, Peters PE. Screening for asymptomatic early bronchogenic carcinoma with low dose CT of the chest. Cancer 2000; 89(11 Suppl):2483–2484.